

Influence of net doping, excess carrier density and annealing on the boron oxygen related defect density in compensated n-type silicon

F. E. Rougieux,^{1,a)} B. Lim,² J. Schmidt,² M. Forster,^{1,3,4} D. Macdonald,¹ and A. Cuevas¹¹Research School of Engineering, College of Engineering and Computer Science, The Australian National University, Canberra ACT 0200, Australia²Institute for Solar Energy Research Hamelin (ISFH), Am Ohrberg 1, D-31860 Emmerthal, Germany³Apollon Solar, 66 cours Charlemagne, 69002 Lyon, France⁴INSA de Lyon, INL, 7 av. J. Capelle, 69621 Villeurbanne Cedex, France

(Received 16 May 2011; accepted 28 July 2011; published online 20 September 2011)

In this study, we present experimental data regarding the concentration of the boron-oxygen complex in compensated n-type silicon when subjected to illumination. We find that the defect density is independent of the net dopant concentration and is strongly dependent on the minority carrier concentration during illumination. We show that annealing at temperatures in the range 500 °C to 700 °C permanently reduces the defect density possibly via a decrease in the oxygen dimer concentration. © 2011 American Institute of Physics. [doi:10.1063/1.3633492]

I. INTRODUCTION

Combining the advantages of upgraded metallurgical grade silicon (low cost and embodied energy) and the greater immunity to impurities of n-type silicon, boron-phosphorus compensated n-type silicon is a promising material for solar cells. However, it has recently been shown to degrade due to boron-oxygen (BO) related light induced degradation (LID),^{1–4} which is very well known in boron doped p-type silicon.^{5,6}

Lim *et al.*² revealed the slow kinetics, compared to p-type silicon, of both the generation and the annihilation of the defect in compensated n-Si. They also showed that the defect generation and annihilation processes could not be fitted by a simple exponential function as is the case in p-type silicon. Geilker *et al.*⁴ proposed that the defect concentration depends on the compensation ratio rather than the net doping or the boron concentration. Schutz-Kuchly *et al.*³ showed the defect to have a smaller impact on cell efficiency in compensated n-type than in compensated p-type silicon. However, much remains to be understood about the boron-oxygen complex formation mechanism in compensated n-type silicon. In particular, the effect of net doping on the defect density remains unclear, although it is essential to determine this to assess the suitability of compensated n-type Si for solar cell fabrication.

In p-type silicon, Bothe *et al.*⁷ and Glunz *et al.*⁸ have shown that the defect density can be reduced by a high temperature thermal process (>700 °C). Bothe *et al.*⁷ also demonstrated a reduction of the defect density by thermal donor creation at low temperature (at 450 °C dimers transform to longer oxygen chains). However, the effect of intermediate temperature annealing (500 °C to 700 °C) remains unknown.

In this paper, we investigate the effect of net doping on the BO defect density in n-type compensated silicon using

carrier lifetime measurements. We demonstrate that the BO defect density is independent of the net doping and also show that the defect density is approximately proportional to the excess carrier density during illumination. We then explore the effect of intermediate temperature annealing on the BO defect density and show that a permanent reduction of the defect density can be obtained by such annealing. Finally, we analyze the implications of our findings for a recent BO model⁹ and for the potential of compensated n-type silicon as a material for solar cells.

II. EXPERIMENTAL METHODS

The samples used in this study were from a single compensated Cz-Si ingot doped with both boron and phosphorus. The boron and phosphorus concentrations were measured by secondary ion mass spectrometry (SIMS). The net doping was measured by electrochemical capacitance voltage (ECV) measurements. The interstitial oxygen concentration was measured using Fourier transform infrared spectroscopy (FTIR) and was found to be between $6 \times 10^{17} \text{ cm}^{-3}$ and $9 \times 10^{17} \text{ cm}^{-3}$. Figure 1 shows the boron, phosphorus, net doping, and interstitial oxygen concentrations along the length of the ingot. Both the segregation coefficient and initial dopant concentrations in the melt were varied in order to fit the SIMS profile. We found segregation coefficients of $k_B = 0.75$ and $k_P = 0.41$ for boron and phosphorus, respectively. The initial boron concentration was found to be approximately $[B] = 6.2 \times 10^{16} \text{ cm}^{-3}$ and the phosphorus concentration $[P] = 1.1 \times 10^{17} \text{ cm}^{-3}$. Only samples from the n-type part of the ingot were used in this study.

The samples were damage-etched and RCA cleaned. To study the impact of net doping on the defect density, a first batch of samples with a range of net doping values from $5.7 \times 10^{15} \text{ cm}^{-3}$ to $4.0 \times 10^{16} \text{ cm}^{-3}$ was then subjected to a phosphorus diffusion step to remove fast-diffusing impurities that can affect the lifetime. The gettering layer was then etched in HF/HNO₃. To assess the influence of thermal treatment on the defect density, a second batch of samples, all

^{a)}Author to whom correspondence should be addressed. Electronic mail: fiacre.rougieux@anu.edu.au.

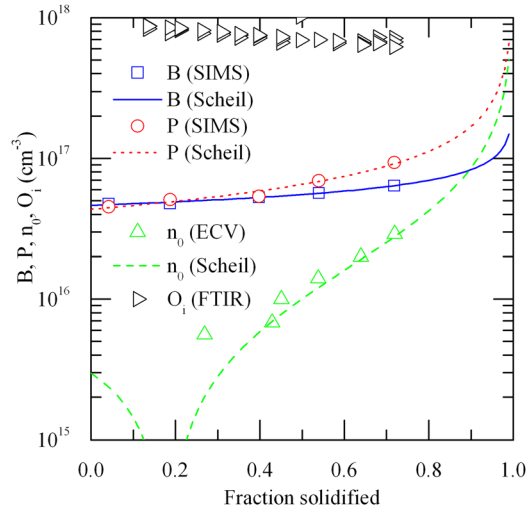


FIG. 1. (Color online) Ingot profile showing boron, phosphorus, net doping, and interstitial oxygen concentration. The solid lines are fits to the data using Scheil's equation.

with similar net doping ($n_0 = 3 \times 10^{15} \text{ cm}^{-3}$), were annealed for 1 h at different temperatures from 500 °C to 700 °C in a quartz furnace tube under nitrogen flow. All samples were then RCA cleaned and coated at 450 °C with plasma-enhanced chemical vapor-deposited silicon nitride. The BO defect has been shown previously to deactivate very slowly in compensated n-type Si.² To ensure full deactivation, the samples were annealed at 200 °C for 100 h. The samples were then degraded under various light intensities and temperatures.

Effective lifetime measurements were performed using the quasi-steady-state photoconductance technique (QSSPC).¹⁰ The measured lifetime after full deactivation is referred to as τ_{annealed} while the degraded lifetime is τ_{degraded} . The lifetime measured was extracted at a fixed injection level equal to 10% of the net doping n_0 . The effective defect concentration was then determined as $N_t^* = 1/\tau_{\text{degraded}} - 1/\tau_{\text{annealed}}$. QSSPC measurements are sensitive to the mobility sum, and mobility reductions have been observed before in compensated silicon.¹¹ Therefore we used the sum of acceptor and donor concentrations from the fit to the SIMS data as the input parameter of the mobility model (Dannhauser and Krauss)^{12,13} to obtain reasonable values of the lifetime.¹¹

III. RESULTS AND DISCUSSION

The classical boron-oxygen model¹⁴ involves a substitutional boron B_s and an oxygen dimer O_{2i} . In this model, a mobile positively charged oxygen dimer O_{2i}^+ is thought to diffuse at room temperature through the capture of holes and electrons, until reaching a negatively charged substitutional boron atom B^- .¹⁵ The interstitial oxygen concentration $[O_i]$ is known to have a quadratic influence on the dimer concentration¹⁶ and thus on the BO defect density.^{5,14,17} Therefore the concentration of B_sO_{2i} created is proportional to the boron concentration and quadratically related to the interstitial oxygen concentration ($N_t \propto N_A \times [O_i]^2$). The validity of the classical boron-oxygen model was questioned when it was shown that the defect density depended on the net doping

($N_t \propto p_0 \times [O_i]^2$) rather than the total boron concentration ($N_t \propto N_A \times [O_i]^2$) in compensated p-type silicon.^{18,19} The BO defect generation rate was also shown to have a quadratic dependence on the net doping ($R_{\text{gen}} \propto p_0^2$).²⁰ Moreover Murin *et al.*²¹ have recently shown that diffusion of oxygen dimers is not expected to occur at room temperature, thus an alternative model for the BO defect is needed.

To explain the defect density dependence on the net doping Voronkov *et al.*⁹ presented an alternative model involving interstitial boron B_i rather than substitutional boron B_s . In this model, the oxygen dimers are not mobile at room temperature but bind to the interstitial boron during ingot cooling. The concentration of B_iO_{2i} then depends on the B_i concentration at the freeze-in temperature, which in turns depends on the net doping at the freeze-in temperature ($N_t \propto p_0 \times [O_i]^2$). This state of the B_iO_{2i} defect is thought to be latent and is subsequently transformed into a recombination active defect under illumination. Macdonald *et al.*¹⁹ presented an alternative model involving interstitial boron B_i binding with mobile oxygen dimers at room temperature. Both of these models predict the defect density to be inversely proportional to the net doping in n-type silicon and to be independent of the light intensity during defect generation.

In this work, we investigate the key factors that determine the defect concentration and the defect generation in compensated n-type samples and compare our findings to the models mentioned above. In addition, we investigate thermal treatment as means to reducing the defect density.

A. Influence of the net doping

Figure 2 shows the lifetime τ evolution during the defect formation for three compensated n-type Si samples with different net doping under an illumination intensity of 60 mW/cm². Also shown is a control non-compensated 1 Ω .cm n-type Cz silicon sample the lifetime of which remains constant, thus confirming that the surface passivation is stable and does not affect the changes observed in the other samples. Interestingly, the lifetime of the different

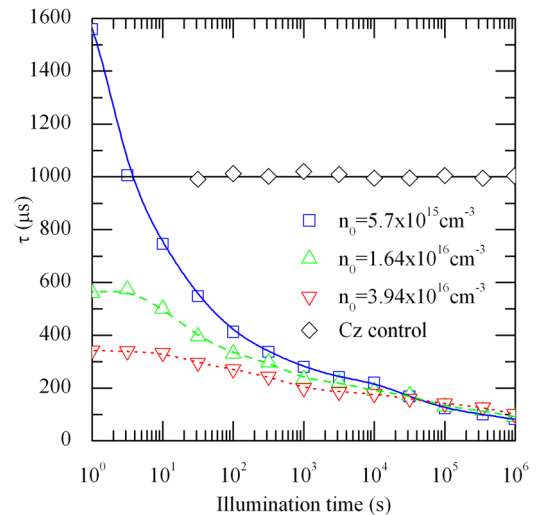


FIG. 2. (Color online) Evolution of the lifetime during light induced degradation for three samples with different net doping levels ($G = 60 \text{ mW.cm}^{-2}$, $T = 60^\circ\text{C}$). The lines are guides to the eye.

compensated samples crosses over at one point. Note that the degradation is not completely saturated, even after more than 1 month of illumination, reflecting the much slower formation rates compared to p-type silicon. However, because the interstitial oxygen concentration decreases along the ingot, the effective defect concentration should be normalized by the square of the interstitial oxygen concentration to allow for proper comparison between the samples. Figure 3 shows this normalized effective defect density as a function of the net doping after different illumination times. The defect density after a given time appears to be approximately independent of the net doping, indicating that the rate of defect creation is very similar for all net doping values.

B. Impact of excess carrier density during illumination

For this study, the BO defect has been generated using different light intensities. The light induced degradation process has already been shown to be an electronically induced degradation mechanism and as such it is the excess carrier density, rather than the light intensity itself, that creates the defect.

A simple way to determine the excess carrier density in a sample under a given generation rate is to measure the carrier lifetime, in this case using an inductive coil. The carrier lifetime is given by $\tau = \Delta n / G$, with Δn being the excess carrier density in the samples and G the generation rate. Combining the intensity of the bias light during the degradation and the optical properties of the sample, one can easily determine the carrier generation rate G in the sample. Using the lifetime measurement τ and the generation rate G , one can obtain the excess carrier density in the sample during the BO generation $\Delta p_{\text{generation}}$. A temperature controlled inductive coil photoconductance setup was used to measure the excess carrier density in this way at 60 °C.²²

Figure 4 shows the evolution with time of the carrier lifetime and the implied open-circuit-voltage V_{OC} , for two different degradation light intensities at 60 °C. The implied V_{OC} is calculated via the excess carrier density measured

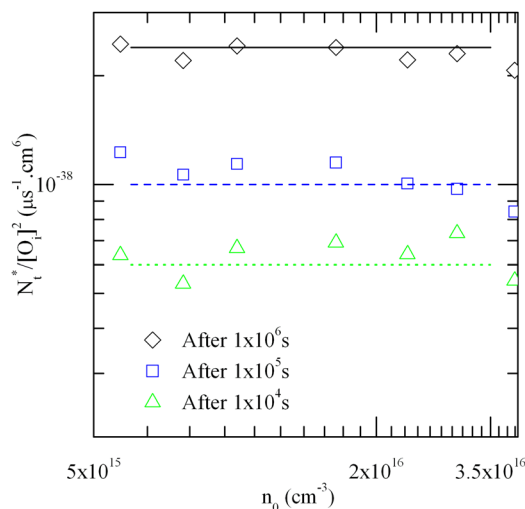


FIG. 3. (Color online) Normalized effective defect density as a function of the net doping after different illumination times (1×10^4 s, 1×10^5 s, and 1×10^6 s). The lines are guides to the eye.

under an illumination intensity corresponding to 1 sun (100 mW/cm^{-2}) and reflects the expected impact of the defect on cell performance. Note that the injection level for the implied 1-sun V_{OC} conditions will usually be quite different to that at which the lifetime is reported in Fig. 4. The plot shows that the defect causes a very significant reduction in both the carrier lifetime and 1-sun implied V_{OC} , meaning that such material would be less suitable for high efficiency solar cells than non-compensated n-type silicon without any mitigation of the defect.

In p-type silicon, the injection level during BO generation $\Delta n_{\text{generation}}$ is known to have little effect on the BO defect density N_t^* except for very low injection levels²³ for which the defect formation rate increases with injection. Specifically, the kinetics of the slow forming defect formation are known to saturate for light intensities greater than 1 mW.cm^{-2} in p-type silicon.²³ In contrast, Fig. 4. shows that n-type samples degrade faster under a greater light intensity (60 mW.cm^{-2} compared to 8.5 mW.cm^{-2}), contrary to p-type silicon. Moreover our data indicate that not only the defect generation rate increases with injection but perhaps also the final defect density.

To further confirm this, Fig. 5 displays the effective defect density as a function of excess carrier density during degradation for three different samples after 1×10^5 s and 1×10^6 s of illumination. Note that the samples in Fig. 5 have the same oxygen concentration, therefore the effective defect density is not normalized by the interstitial oxygen concentration. Two samples were degraded at 60 °C with light intensities of 8.5 mW.cm^{-2} and 60 mW.cm^{-2} and one at 30 °C with a light intensity of 8.5 mW.cm^{-2} . The excess carrier density during degradation was determined as described previously. Even if the degradation is not fully completed after these times, this graph suggests that the defect density increases with the minority hole concentration injected during degradation.

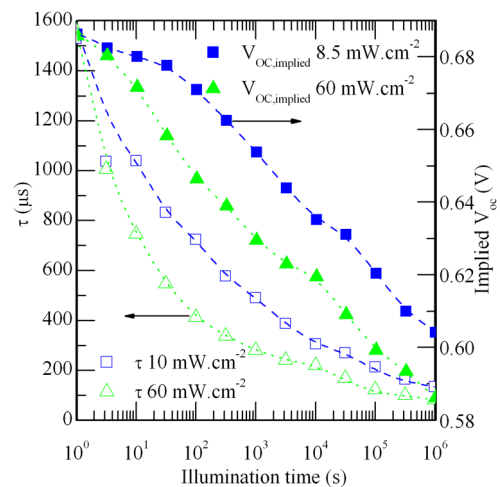


FIG. 4. (Color online) Evolution of the lifetime (empty symbols) and the implied $V_{\text{OC,1Sun}}$ (filled symbols) during light induced degradation at 60 °C for two different light intensities ($n_0 = 5.7 \times 10^{15} \text{ cm}^{-3}$). The lines are guides to the eye.

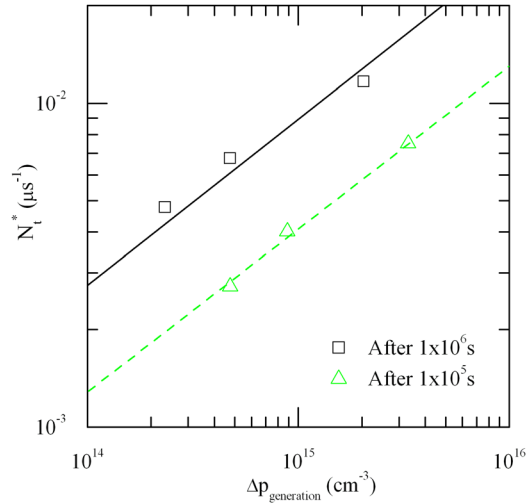


FIG. 5. (Color online) Effective defect density as a function of excess carrier density during degradation for three different samples with the same net doping after 1×10^5 s and 1×10^6 s of illumination. The lines are guides to the eye.

C. Reducing the defect concentration through annealing

The results in the preceding text show that the defect density appears to be independent of the net doping and perhaps also the boron concentration (although this is less clear due to the much weaker variation in the boron concentration in our samples). This would mean that, unlike p-type silicon, lower defect densities may not be readily obtained by reducing the net doping in n-type compensated silicon. Therefore controlling the oxygen dimer concentration could be a useful approach to reducing the defect density. Murin *et al.*¹⁶ have demonstrated that in the 500 °C to 700 °C temperature range the oxygen dimer concentration is reduced through dissociation (without affecting the interstitial oxygen concentrations). Therefore we have performed an experiment to assess this possible way of controlling the defect density.

Figure 6 shows the annealing temperature dependence of the effective defect density N_t^* after a month of illumination (2.7×10^6 s). All of the samples had the same net doping ($5.7 \times 10^{15} \text{ cm}^{-3}$) and the same interstitial oxygen concentration. The 400 °C corresponds to samples that were not annealed but coated with SiN. Annealing between 500 °C and 700 °C reduces the effective defect density. Note that the interstitial oxygen concentration measured by FTIR before and after annealing was not found to decrease significantly (at 700 °C where the highest reduction in interstitial oxygen concentration is expected the oxygen concentration was found to decrease from $[O_i]_{\text{initial}} 8.8 \times 10^{17} \text{ cm}^{-3}$ to $[O_i]_{\text{annealed}} 8.5 \times 10^{17} \text{ cm}^{-3}$).

Analyzing Fig. 6 using an Arrhenius law, we determine an activation energy of $E_a = 0.14 \pm 0.16, -0.04$ eV. Using low temperature FTIR, Murin *et al.* found a dimer binding energy $E_b = 0.3$ eV. Those two activation energies are significantly different; however, there is a large uncertainty in our determination of the activation energy. Therefore it is hard to conclude whether the defect reduction is due partly to the dimer dissociation or if other mechanisms are dominant. This could be partially due to the fact that the samples are

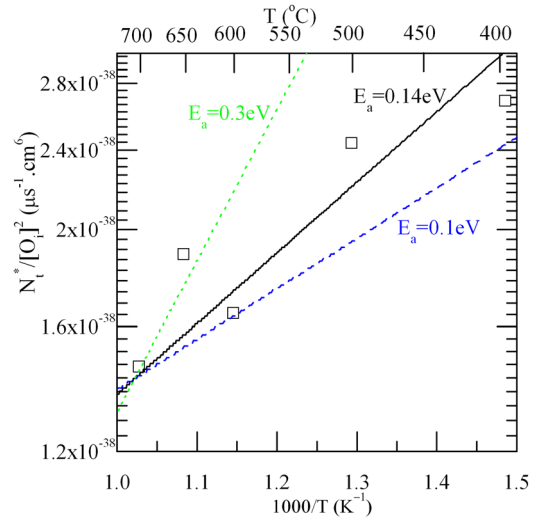


FIG. 6. (Color online) Effective defect density as a function of the annealing temperature for a 1 h anneal. The solid line is a fit using the Arrhenius law.

not completely degraded, even after a month of illumination. Nevertheless, the results demonstrate that annealing in the 500 °C to 700 °C range leads to lower defect densities, a conclusion which should also be valid for p-type silicon.

D. Discussion

Based on our experimental measurements, it is possible that either the defect generation rate is affected by the excess carrier density during BO generation and/or the final defect density itself is affected by the excess carrier density during illumination.

If we assume that only the generation rate is affected by the excess carrier density during illumination, then our observation could be explained within Voronkov's model where the BO defect needs two excess holes to form thus $R_{\text{gen}} \propto \Delta p^2$.

However, Fig. 4. strongly suggests that not only the generation rate is dependent on the excess carrier density but also the final defect density. If that is the case, this would mean that the defect density is not determined during ingot cooling but is determined at room temperature by the Fermi or quasi-Fermi level for holes. This is difficult to reconcile with Voronkov's model in which the defect density should not be affected by the excess hole density during illumination. A further apparent discrepancy with the model is that the defect density seems to be independent of the net doping. This can not be explained by Voronkov's model, where the defect density in n-type compensated silicon should be inversely proportional to the net doping.¹⁹

Another potential explanation is that we are not observing the slow forming defect described by the Voronkov's model, but we are measuring the equivalent of the fast forming defect in n-type compensated silicon. This is supported by the fact that the defect density of the fast forming defect in p-type silicon has previously been shown to increase with the injected carrier density.¹⁴ This could mean that the BO defect formation in compensated n-type silicon could be due to the charging of a latent B_5O_{2i} defect followed by a

thermally activated structural change, similar to the fast forming center in p-type silicon.¹⁴

As seen in the preceding text, the fact that there is a reduction of the BO effective defect density after annealing in the 500 °C to 700 °C range could be partially due to dissociation of the oxygen dimers. This would lead to fewer dimers available to bind with the boron atoms and thus a lower defect density. In practice, this confirms that any high temperature step will permanently reduce the BO defect density. As mentioned in the preceding text, it has previously been demonstrated that a diffusion step (700 °C to 1050 °C) can significantly reduce the defect density.^{8,17} In such thermal processes, both interstitial oxygen clustering and oxygen dimer dissociation are likely to play a role in the reduction of the available oxygen dimer concentration. Therefore any further thermal process at lower temperature (such as a firing step at 700 °C) may increase the defect density again, due to partial dimer re-pairing, although it should still remain lower than the value obtained with no thermal processing. Within *Voronkov's* model there is also the possibility that annealing in the temperature range of 500 °C to 700 °C affects the interstitial boron clusters, which play a key role in determining the defect density.

IV. CONCLUSION

In summary, our results indicate that the net defect density during defect formation does not depend on the net doping in compensated n-type silicon. Moreover, either the generation rate and/or the final defect density appears to depend on the excess carrier density during illumination. If the latter is true, it could mean that the defect density is not fixed during ingot cooling as proposed in recent models^{9,19} but rather fixed at room temperature by the Fermi level (in p-type) or quasi-Fermi level (in n-type) for holes. Our results also show that the defect causes a very dramatic reduction in the carrier lifetime (by approximately an order of magnitude), and implied 1-sun open-circuit voltage, which could potentially make the material unsuitable for high efficiency devices. However, further experiments are needed to confirm and more precisely quantify the relationship among defect density, defect generation rate, and excess carrier density during illumination. Finally, we also demonstrate that annealing between 500 °C and 700 °C effectively reduces the boron-oxygen defect concentration with dimer dissociation

being a possible explanation. Combined with previous work showing defect reductions after higher temperature anneals, this shows that in practice, the defect density can be permanently reduced by almost any high temperature step.^{7,8}

ACKNOWLEDGMENTS

This work was supported by the Australian Research Council (ARC). Thanks are due to Pheng Phang for assisting with sample preparation.

- ¹T. Schutz-Kuchly, J. Veirman, S. Dubois, and D. R. Heslinga, *Appl. Phys. Lett.* **96**, 093505 (2010).
- ²B. Lim, F. Rougieux, D. Macdonald, K. Bothe, and J. Schmidt, *J. Appl. Phys.* **108**, 103722 (2010).
- ³T. Schutz-Kuchly, S. B. Dubois, J. Veirman, Y. Veschetti, D. Heslinga, and O. Palais, *Phys. Stat. Sol. A* **208**, 572 (2010).
- ⁴J. Geilker, W. Kwapil, and S. Rein, *J. Appl. Phys.* **109**, 053718 (2011).
- ⁵J. Schmidt and K. Bothe, *Phys. Rev. B* **69**, 024107 (2004).
- ⁶S. Rein and S. W. Glunz, *Appl. Phys. Lett.* **82**, 1054 (2003).
- ⁷K. Bothe, J. Schmidt, and R. Hezel, in *Photovoltaic Specialists Conference, 2002. Conference Record of the Twenty-Ninth IEEE*, IEEE, New York (2002), p. 194.
- ⁸S. W. Glunz, S. Rein, J. Y. Lee, and W. Warta, *J. Appl. Phys.* **90**, 2397 (2001).
- ⁹V. V. Voronkov and R. Falster, *J. Appl. Phys.* **107**, 053509 (2010).
- ¹⁰R. A. Sinton and A. Cuevas, *Appl. Phys. Lett.* **69**, 2510–2512 (1996).
- ¹¹F. E. Rougieux, D. Macdonald, and A. Cuevas, "Transport properties of p-type compensated silicon at room temperature," *Prog. Photovolt: Res. Appl.* (in press).
- ¹²F. Dannhäuser, *Solid-State Electron.* **15**, 1371 (1972).
- ¹³J. Krause, *Solid-State Electron.* **15**, 1377 (1972).
- ¹⁴K. Bothe and J. Schmidt, *J. Appl. Phys.* **99**, 013701 (2006).
- ¹⁵J. Adey, R. Jones, D. W. Palmer, P. R. Briddon, and S. Oberg, *Phys. Rev. Lett.* **93**, 055504 (2004).
- ¹⁶L. I. Murin, T. Hallberg, V. P. Markevich, and J. L. Lindstrom, *Phys. Rev. Lett.* **80**, 93 (1998).
- ¹⁷K. Bothe, R. Sinton, and J. Schmidt, *Prog. Photovolt: Res. Appl.* **13**, 287 (2005).
- ¹⁸R. Kopecek, J. Arumughan, and K. Peter, in *Proceedings of the 23rd European Photovoltaic Solar Energy Conference*, Valencia, Spain (WIP-Renewable Energies, Munich, Germany, 2008).
- ¹⁹D. Macdonald, A. Liu, A. Cuevas, B. Lim, and J. Schmidt, *Phys. Stat. Sol. A* **208**(3), 559 (2011).
- ²⁰D. Macdonald, F. Rougieux, A. Cuevas, B. Lim, J. Schmidt, M. Di Sabatino, and L. J. Geerligs, *J. Appl. Phys.* **105**, 093704 (2009).
- ²¹L. I. Murin, E. A. Tolkacheva, V. P. Markevich, A. R. Peaker, B. Hamilton, E. Monakhov, B. G. Svensson, J. L. Lindstrom, P. Santos, J. Coutinho, and A. Carvalho, *Appl. Phys. Lett.* **98**, 182101 (2011).
- ²²B. B. Paudyal, K. R. McIntosh, D. H. Macdonald, B. S. Richards, and R. A. Sinton, *Prog. Photovolt: Res. Appl.* **16**, 609 (2008).
- ²³H. Hashigami, Y. Itakura, and T. Saitoh, *J. Appl. Phys.* **93**, 4240 (2003).